Measuring T_g in Ultra-Thin Polymer Films With an Excimer Fluorescence Technique

C. C. WHITE*, K. B. MIGLER, *and* W. L. WU

National Institute of Standards and Technology
Polymers Division
Gaithersburg, MD 20899-8541

An excimer fluorescence technique has been applied to the measurement of T_g of ultra-thin polystyrene films. This technique utilizes an excimer-forming molecule with fluorescent emission in two wavelength bands. The intensity ratio of these bands is a sensitive measure of local viscosity. This technique has been applied to five polystyrene films in the thickness range of 25 nm to 200 nm supported on quartz substrates. The observed T_g for the five ultra-thin polymer films was similar to the bulk T_g with no observed dependence upon thickness. Additionally, the T_g determined for each film did not show any dependence upon thermal history.

INTRODUCTION

The dynamics of ultra-thin polymer films is currently the subject of intense fundamental and technological interest. Fundamentally, this size scale is commensurate with the unperturbed dimension of a single polymer molecule. Thus, a large portion of the molecules will be in close proximity to an interface. This interface affects the dynamics of the polymer and the physical properties of the film. Technologically, a continual size reduction of polymeric components used to assemble integrated semiconductors is driven by the demand for faster clock speeds and increased processing power. The newest commercial microprocessor incorporates 180 nm features (1). The ability to accurately predict the reliability of these electronic packages depends upon a precise determination of the material properties, such as the glass transition temperature, T_g (2).

Recent studies by a variety of techniques have concluded that the T_g of ultra-thin polymer films can exhibit thickness-dependent variations from bulk values (3–6). For polymers in contact with surfaces that have a specific favorable interaction, there is general agreement that the glass transition temperature increases (3). However, if the polymer is next to surfaces with no specific interaction, there are reports that the T_g of the polymer either increases (5, 6), decreases (3, 4), or stays the same (7, 8). The majority of these studies have employed ellipsometry or X-ray reflectivity techniques to measure changes in the film thickness as a function of temperature. These techniques measure a coefficient of thermal expansion (CTE), which exhibits a change in slope at the glass transition temperature.

Other studies have concentrated on local scale dynamics (7–12). Torkelson *et al.* (7) used second harmonic generation to probe the segmental mobility associated with the α-relaxation mode and observed broadening in the distribution of relaxation times in thin films. In another study, Torkelson *et al.* used nonradiative energy transfer to measure translational diffusion of a probe and observed decreases in a PS matrix below 150 nm (8).

The excimer technique described in this paper has important advantages and distinctions compared to other methods. Most critically, it is sensitive to the local scale dynamics. Additionally, this technique is simpler than the optical probe diffusion studies that require covalent binding of the fluorescent molecule to the polymer, preparation of bilayers and the limitation of one data point per prepared bilayer film. Other important advantages include the ability to work in a variety of geometries such as buried interfaces, free-standing films and non-planar interfaces, e.g. particles. It can also be applied to high-pressure environments.

Since the viscosity of polymer melts changes widely in the vicinity of T_g, by employing a viscosity sensitive fluorescent probe, we were able to determine the T_g of polymer films in the thickness range of 25 nm to 200 nm supported on a quartz substrate. The theory of this experimental design, instrument construction, and results from tests with five polystyrene films are presented in this paper.

*Corresponding author.

FLUORESCENCE DESCRIPTION

Figure 1 illustrates 1-3-bis-(1-pyrenyl)propane (BPP), the fluorescent probe molecule employed in these studies. The physics of this fluorescent probe system has been described in detail elsewhere (13–16), but a brief summary is given here. It consists of two pyrene groups connected by a three-carbon aliphatic chain. Spectroscopically, it absorbs at 345 nm to 350 nm and has two principal fluorescence emission wavelengths: 380 nm–400 nm (monomer emission) and 450 nm to 550 nm (excimer emission). The 345 nm excitation corresponds to the absorbance of a photon by one pyrene group. The excited state can reemit a photon at its characteristic fluorescence wavelength of 380 nm to 400 nm without interaction with the second pyrene; this is the monomer emission. A second process occurs when the excited and ground state pyrene groups bend about their flexible aliphatic linkage, come into close physical proximity and interact electronically to form an excimer state. Fluorescence from this state is termed excimer fluorescence and occurs at longer wavelength 450 nm to 550 nm.

In order for the excimer state to form, the two pyrene groups must rearrange before the excited one decays to the ground state via monomer fluorescence. The local viscosity of the medium is a controlling factor for this rearrangement. Thus, the excimer to monomer fluorescence ratio is sensitive to the local viscosity. If the viscosity is high, then rearrangement is slow and there will be little excimer fluorescence. As the viscosity decreases as T_g is crossed, then excimer formation and its subsequent fluorescent emission are possible. At the elevated temperatures typical of polymer melts, the dissociation of the excimer state to the monomer becomes important as well (17).

The relatively large volume required to form the eximer fluorescence of the BPP chromophore is critical for the sensitivity of the fluorescence intensity ratio to the viscosity of the surrounding polymer molecules. This sensitivity model of the fluorescence intensity ratio of the BPP is supported by measurements relating the change in the fluorescence intensity ratio to the free volume of the polymer matrix (9, 13–15, 18–20). Further evidence is found in a paper by Bur *et al.* (16); In this paper two probes were incorporated within a polymer matrix, the relatively large BPP and a much smaller probe, (1(4-dimethylamino)-6-phenyl-1,3,5 hexatriene) or DMA-DPH. Fluorescence measurements as a function of temperature on this sample demonstrated that the BPP was sensitive to the matrix viscosity whereas the smaller DMA-DPH was not. With this foundation it is not unexpected that the temperature dependence of the ($I_{monomer}/I_{excimer}$) ratio exhibits a WLF temperature dependence above the glass transition temperature (16).

A critical property of the BPP/polymer matrix system is that it is independent of the total fluorescence intensity, for suitably low dye concentration. One is only interested in the ratio of the monomer to excimer fluorescence. This property greatly simplifies the interpretation of the experimental data. The specific value of the ($I_{monomer}/I_{excimer}$) ratio is somewhat arbitrary, it is a function of the optics of the system (example: width of bandpass filters) and the specific alignment. The important quantity is not the absolute value of the ($I_{monomer}/I_{excimer}$) ratio, but the temperature

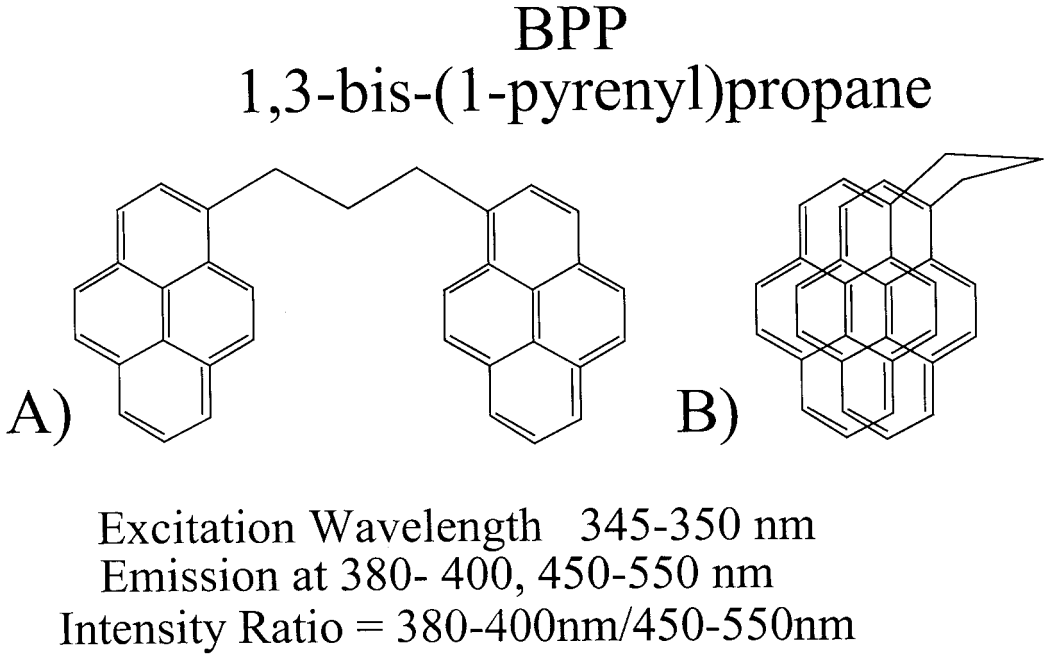

Fig. 1. Molecular structure of the excimer forming 1-3-bis-(1-pyrenyl)propane dye. The two conformations of the dye molecule: A) Monomer, emission wavelength is 380–400 nm, and B) Excimer emission wavelength is 450 nm to 550 nm.

dependence which is clearly discernable. It is important to evaluate the changes in the fluorescence profiles as a function of temperature as a careful check on the assumption of the relative independence on the total fluorescence intensity. This assumption that any changes in the $((I_{monomer}/I_{excimer})$ ratio results directly from changes in the polymer matrix and not from changes in the fluorescence profiles with temperature has been carefully evaluated for the temperature ranges studied here. If the temperature is increased above the ranges studied here, changes in the $(I_{monomer}/I_{excimer})$ ratio cannot be solely attributed to changing viscosity of the polymer matrix.

INSTRUMENT DESIGN

The previous section referred to the basic requirements of the instrument design: excitation of the dye at 345 nm and detection of the fluorescence intensity of the monomer and excimer wavelengths at 380 nm and 450 nm, respectively. Precise temperature control and measurement is also vital for characterizing the glass transition temperature. The instrumental design to accomplish these tasks is illustrated in *Fig. 2*.

The collimated, spectrally filtered, and focused (by a fused silica lens (f = 50 cm) to a spot size of ≈1 mm) emission from an Oriel (21) 75 W Xenon arc lamp was used to excite the chromophore. Sample polymer films containing the chromophore, which were spun onto a quartz disk 2.5 cm in diameter (technique described in **Sample Preparation** section) were placed in the focus of the excitation light.

Detection of the fluorescence intensity was achieved by first using a collection lens (f = 25 cm) and then a focusing lens (f = 25 cm). The total intensity was focused onto the end of a 5-mm-diameter UV-Vis Liquid light guide (Oriel, #77556). The other end of the liquid light guide was connected into a beam splitter (Oriel, #45702). The two light paths were then focused onto one of two identical photomultiplier tubes (PMT, Oriel#77348), powered by a single high voltage power supply (Stanford Research Systems, Inc.) Wavelength selection was achieved by placing band pass filters in front of each tube. The band pass filters were constructed by combining a Newport short pass filter with a long pass filter. For example, the longer wavelength filter was made by combining a 10LWF-400 short pass filter (transmitted range 440 nm to 1320 nm), with a 10SWF-650 long pass filter (transmitted range 400 nm to 614 nm) for a band pass of 440 nm to 614 nm. The voltage signal from each PMT is then passed to each channel of a two channel gated photon counter (Stanford Research Systems SR400). The

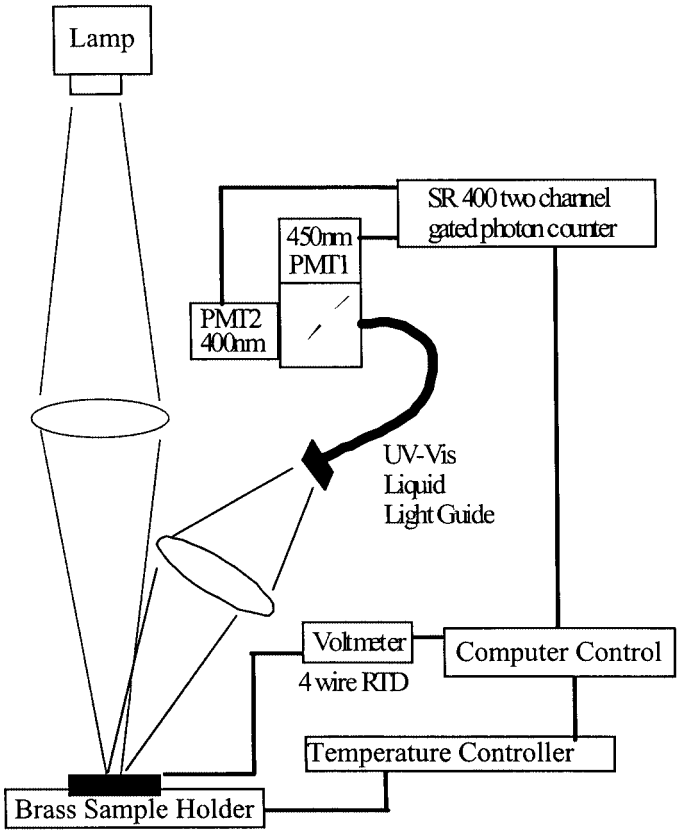

Fig. 2. Experimental setup. The excitation of the chromophore doped polymer film is through a Xenon arc lamp. The two emission wavelengths are collected and detected with a matched pair of photomultiplier tubes. A Watlow controller controls the temperature and an independent 4 wire RTD is used to detect the film temperature.

specific value of the ($I_{monomer}/I_{excimer}$) ratio, recorded from the SR400 is somewhat arbitrary, it is a function of the optics of the system (example: width of bandpass filters), and the specific alignment.

The sample holder is a brass plate, 17.78 × 6.35 × 1.27 cm, which has been drilled to accommodate two equally spaced custom (17.78 cm long × 0.317 cm diameter) firerod cartridge heaters (Watlow). These are controlled by a Watlow 982 PID temperature controller and solid state relay system. A three-wire platinum resistance temperature device (RTD) temperature probe is used to determine the controlling temperature. With this design, the temperature of the brass plate is controlled to the set point better than ±0.03°C and has a stability of better than ±0.01°C. The stability was determined by making repeated measurements throughout the entire temperature range of interest (20°C to 170°C).

The sample was coated on the surface of a quartz disk that is in contact with the brass block. Quartz was chosen as the substrate because of two principal advantages, the high transparency in the wavelengths of interest and the reproducibility of the surfaces. The quartz disk placed on the brass plate with a small amount of Dow Corning 340 silicone heat sink compound. In order to accurately determine the temperature of the polymer film, a thin four-wire platinum RTD (Omega TFD) was attached to the film with conductive paste, away from the excitation focus point. The resistance on this second RTD was determined with a Keithley 197A voltmeter. The resistance could be determined to ±0.1 mΩ. The polymer temperatures reported in this study are from this second measurement with measured stability better than ±0.01°C. The experiment was fully automated and utilized a custom Labview® program to communicate with the external devices. In a typical experiment, the starting temperature is set and the system is allowed to come to thermal equilibrium (30 min). The fluorescence intensity of each sample is integrated for 10 s by the SRS 400 for each wavelength range of interest. Multiple data points were collected on each sample, resulting in an average of 24 readings for every degree.

SAMPLE PREPARATION

Solutions of polystyrene (Polymer Laboratories Ltd. Mn = 220,500 g/mol M_w/M_n = 1.02, Batch #201137-8) in toluene were prepared with mass fraction 0.006 to 0.03. To this solution, BPP was added such that a constant mass ratio of 0.1 BPP to polystyrene was maintained for all solution concentrations studied. These solutions were prepared at least 24 h before the films were spun cast. The quartz disks (2.5 cm diameter) were washed in acetone, exposed to an oxygen plasma (Plasmaline) for 15 min, and placed in a UV/Ozone cleaner for 3 min (Jelight #42 UVO). The films were spun onto the cleaned quartz disks within 20 min of the final UV/Ozone cleaning. A Headway Spin Coater was used to spin cast the ultra-thin polymer films. The thickness of the film was set by the concentration of the polymer solution as summarized in *Table 1*. The thickness of the ultra-thin polymer film was determined by X-ray reflectivity on a Scintag (XDS 2000). This technique involves determining the thickness by constructing a model electron density profile and experimentally determining the intensity of the reflected X-rays as a function of the scattering vector, q ($q = 4\pi/\lambda(sin\theta)$) where λ is the wavelength and θ is the specular reflection angle). This model profile prediction is then compared to the experimental determination of the specular reflected X-Ray intensity versus q. The model is then modified until a "best-fit" match of the experimental data and model prediction is achieved. The experimental thickness of the ultra-thin polymer films is assumed to be identical to the model layer thickness. The details of this technique are presented elsewhere (5). The thickness was determined with an expanded uncertainty of ± 0.2 nm. The experimental data, calculated model fit, and electron density model are shown for the (68.7 ± 0.2) nm polystyrene film in *Fig. 3*.

Table 1. The Concentration of Polystyrene/Toluene Solution and the Resulting Film Thickness Determined With X-Ray Reflectivity. The Standard Uncertainty for the Mass Fraction is 4×10^{-5}.

Mass Fraction ×100	Film Thickness, nm ± 0.2 nm
3.311	215.3
1.878	76.3
1.500	68.7
1.103	45.8
0.660	25.3

RESULTS AND DISCUSSION

The glass transition temperature of the polystyrene with BPP probe was determined independently by using a differential scanning calorimeter with a heating rate of 10°C/min (calibrated versus Indium at the same heating rate). The resulting data exhibit an expected transition centered at 100°C (calculated by midpoint method).

In a typical excimer fluorescence experiment, the starting temperature is set and the system equilibrates for 30 min. The fluorescent intensity was integrated for 10 s for both wavelength bands during the temperature scans. In order to study the effect of thermal history, the samples were cycled at least six times from 60°C to 130°C with a heating/cooling rate of 0.25°C/min.

The fluorescence intensity ratio ($I_{monomer}/I_{excimer}$) as a function of film temperature is shown in *Fig. 4* for a 68.7 ± 0.2 nm polystyrene film. From this figure, two regions can be identified—a low temperature region where the fluorescence ratio is independent of temperature, and a high temperature region where the fluorescence ratio is a decreasing function of temperature. A linear extrapolation method was chosen as

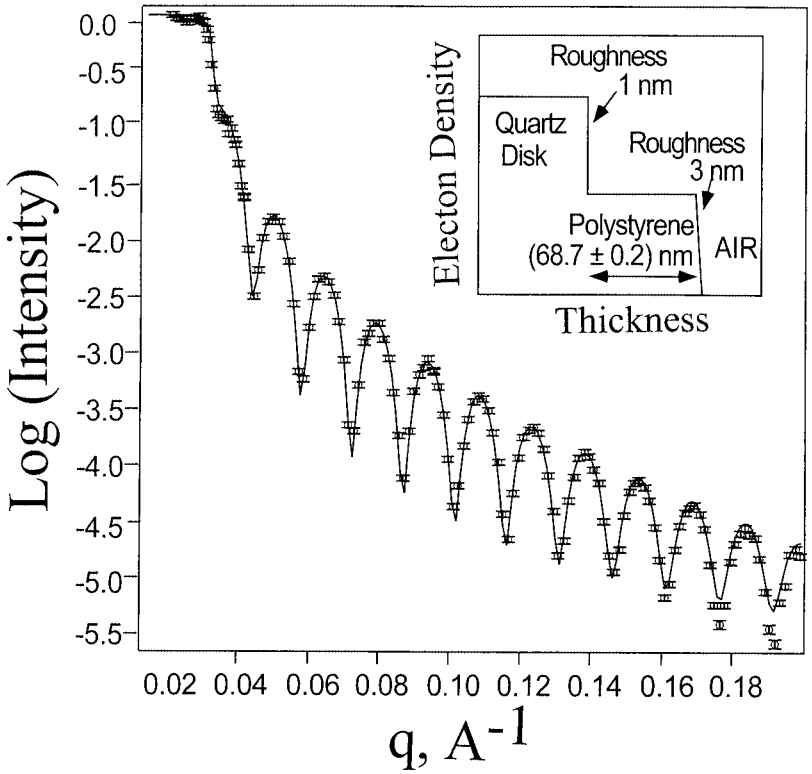

Fig. 3. The X-ray intensity as a function of q or scattering vector. The experimental profile is fitted with a model electron density structure shown as an inset. The presence of fringes in the profile allows for rate thickness determinations. The bars on the data points represent the standard uncertainty of the data points.

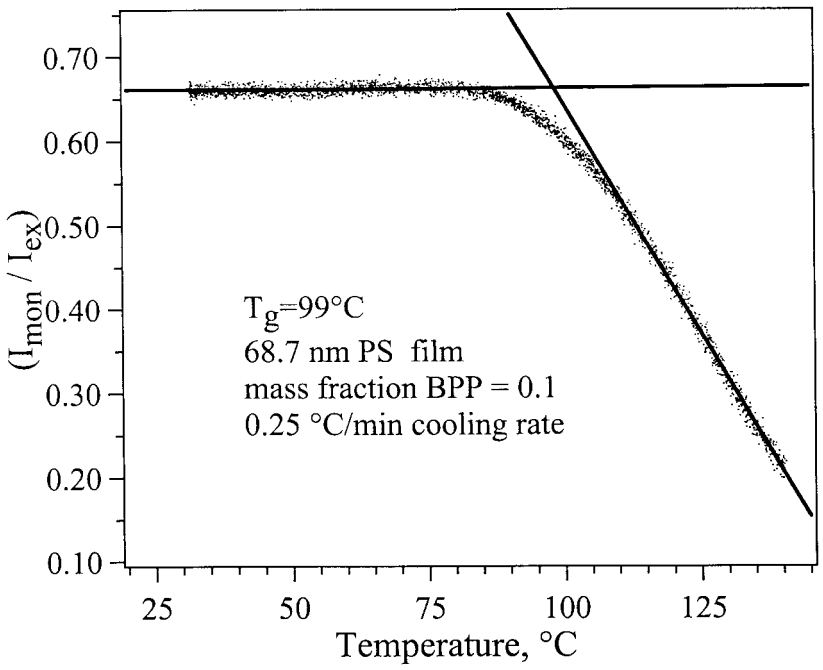

Fig. 4. Measurement of T_g via the excimer fluorescence technique. The fluorescence intensity ratio ($I_{monomer}/I_{excimer}$) as a function of temperature. Two regions are evident, a low temperature region where the ($I_{monomer}/I_{excimer}$) is independent of temperature. In the second higher temperature region, ($I_{monomer}/I_{excimer}$) is a function of temperature. The linear extrapolation method for determining the operational definition of T_g is also shown. The standard deviation of the ratio values is 0.006.

an operational definition of the glass transition temperature for this study. The linear extrapolation method is shown in *Fig. 4* and the resulting T_g is found to be (99 ± 2)°C for the (68.7 ± 0.2) nm polystyrene film. To calculate the uncertainty estimates for this data, extremes of the possible slopes in the region $T < T_g$ and $T > T_g$ were determined. From these lines, four possible intersections were determined and the subsequent variation in the determinations of the operationally defined T_g resulted.

The fluorescence intensity ratio ($I_{monomer}/I_{excimer}$) of each of the five films were measured on both heating and cooling with identical rates, ± 0.25°C/min. This cycle was repeated at least three times for each film, resulting in at least six measures of the operational T_g. The results of this cycling are shown in *Fig. 5a* for the 68.7 nm ± 0.2 nm and *Fig. 5b* for a 25.3 nm ± 0.2 nm polystyrene film respectively. For clarity, a small solid circle is added at the intersection of the two linear extrapolations for that heating/cooling cycle. The curves obtained on heating all give T_g values of (98°C ± 2°C) while a slightly higher T_g of (100°C ± 2°C) was obtained on film cooling. For the 25.3 nm ± 0.2 nm sample, *Fig. 5b*, values of 101°C ± 2°C for heating and 103°C ± 2°C for cooling are observed. Again, the uncertainty estimates for the T_g determination were obtained by procedure outlined in the explanation for *Fig. 4*.

The fluorescence intensity ratio ($I_{monomer}/I_{excimer}$) decreases with each successive thermal cycle. This is due to a photo-bleaching which will be discussed later. In *Fig. 5*, the fluorescence intensity ratio in the temperature-independent region of the first heating cycle has a value of 0.68 and the subsequent cooling cycle has a value of 0.61, which is also the value for the next heating cycle. This successive decrease in the fluorescence intensity ratio is observed for all the temperature cycles. The inset of *Fig. 5* depicts how normalizing the temperature-independent fluorescence ratios results in a single master curve with a T_g of (100 ± 2)°C.

A plot of T_g versus film thickness is presented in *Fig. 6*. For each symbol on this plot, the determinations of T_g, from both heating and cooling, were averaged. The mean and first standard deviation for each thickness is represented on *Fig. 6*. The solid line is the value of T_g obtained from DSC on bulk samples. Also shown on this plot is the value of 3* R_g (the radius of gyration of the polystyrene, calculated from the molecular mass). The values reported for T_g in this study are independent of film thickness within the range of film thickness studied.

The linear extrapolation method, illustrated in *Figs. 4* and *5* was chosen to give an operational definition of T_g for this study. This method has been successfully applied in previous studies on bulk samples of polystyrene (16). Our data has demonstrated that this

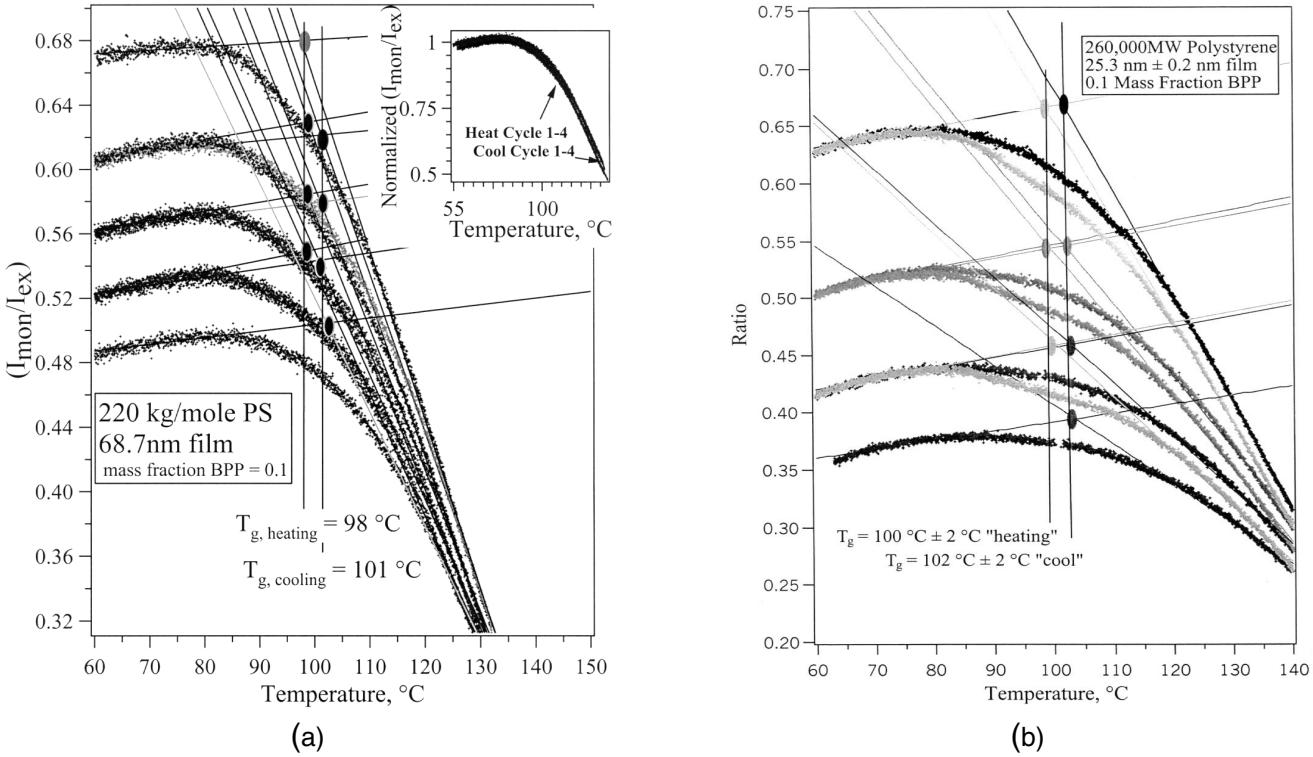

Fig. 5. Eight temperature cycles of the ($I_{monomer}/I_{excimer}$) versus temperature are shown for the (68.7 ± 0.2) nm (Fig. 5a) and a 25.3 nm ± 0.2 nm (Fig. 5b) polystyrene film. The eight determinations from the linear extrapolation method of the glass transition temperature are also shown for each figure. The T_g determined is independent of cycle number. The inset in Fig. 5a shows that for the normalized ($I_{monomer}/I_{excimer}$) ratio, all the curves collapse onto a single master curve. The standard deviation of the ratio values is 0.006.

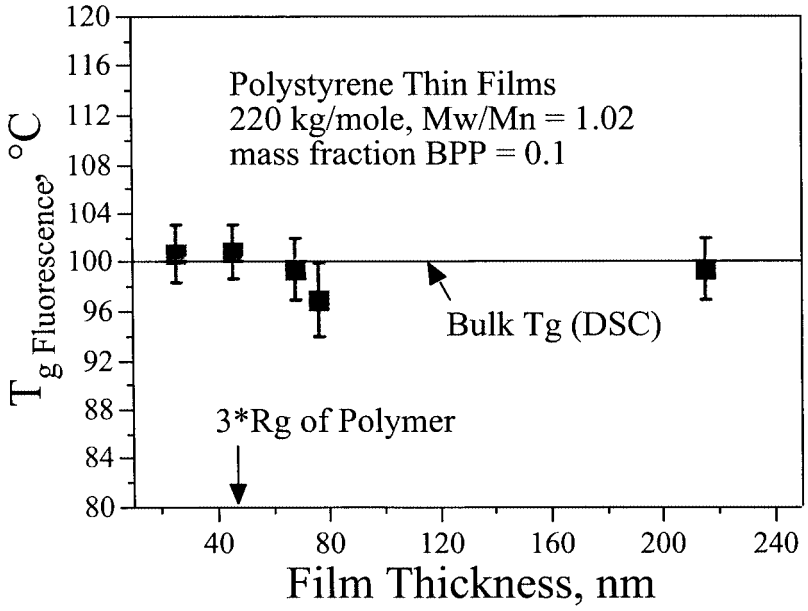

Fig. 6. Glass transition temperature of polystyrene as a function of film thickness. The line represents the value of T_g obtained by DSC. There is no dependence of T_g on the thickness for the five films studied. The data on this graph represents the mean and standard deviation for the determinations of the T_g for each film thickness studied.

technique can successfully be adapted to the ultra-thin film geometry.

A significant concern in studies of ultra-thin polymer films is that of establishing a standardized thermal and stress history. The process of spin coating ultra-thin polymer films may impart significant residual stress to the resulting film. Most studies of ultra-thin films rely on 12 h to 24 h of annealing at temperatures approximately 20°C above the bulk T_g to relax this residual stress and remove residual solvent. There is some question as to whether this actually removes the residual stress in the film (22, 23). To address this concern, a known thermal history was given to the supported polymer films by cycling the heating and cooling, with the film spending 4 h above the measured glass transition temperature during each cycle. It is noted that for each of the films studied, there was no discernable trend in the operational T_g as a function of cycle number (see *Fig. 5*).

Probe segregation is a concern in this study. Some models proposed to explain the deviation from observed bulk behavior suggest different regions of an ultra-thin polymer film may exhibit different glass transition temperatures (24, 25). Experimental evidence from NEXAFS suggests that there is no spatial segregation in ultra-thin films into regions with different T_g behaviors (26). If the chromophore is segregating into one of these proposed regions, then the measured T_g reflects only the properties of that region, and not the entire film. The samples measured in this study were prepared by spin casting as described above. Before spin casting, there was an equilibrium distribution of chromophore and polymer molecules. If it is assumed that the spin casting process does not allow enough time for dye segregation, then the cast film will also have an equilibrium distribution of chromophore. With the high viscosity assumption for the polymer film, the first opportunity for dye segregation would be when the intensity ratio becomes a function of temperature. Since no trend is observed in the measured T_g as a function of cycle number, it can be assumed that the local environment of the chromophore stays unchanged throughout the whole experimental procedure. Recent experiments employing both neutron and X-ray reflectivity on a deuterated polystyrene/ hydrogenated BPP system confirm that the dye does not segregate during this experimental protocol (27).

The decrease in the fluorescence intensity ratio in the temperature-independent region for each thermal cycle is due to a photochemical reaction of the dye. During these experiments, the dye spot is exposed under a constant illumination for approximately 40 hours. If the beam spot is moved to a different location on the sample at the conclusion of the experiment, the initial intensity and ratio are recovered. A separate experiment at constant temperature has shown that there is a slow temporal decline in the fluorescence ratio. This decline can completely account for the vertical offset in the fluorescence intensity ratio between the separate heating and cooling cycles shown in *Fig. 5a* and *5b*. This mechanism is also responsible for a very slight curvature present within each distinct temperature run. Additional experiments, not shown here, have been preformed with a higher rate of temperature change that do not show slight curvature in the data. A third experiment has been preformed where the sample is held at constant

temperature ($T < T_g$) for a several hours. The fluorescence intensity ratio, when plotted as a function of time, shows a slight decrease. When the data for an individual heating or cooling run is plotted as a function of time and corrected by this amount of decrease, this small time, not temperature, dependence, which gives rise to a slight curvature in the data, is eliminated. Each individual temperature run in both *Fig. 5a* and *5b* have been corrected for this slight temporal curvature. This correction does not change the T_g determinations of any of the individual temperature profiles. This is demonstrated by the ability to normalize the fluorescence intensity ratio and collapse all the heating or cooling curves, each with a different level of photodegradation onto a single master heating or cooling curve (see inset of *Fig. 5a*).

The 0.1 mass ratio of the BPP to polystyrene is required to produce measurable temperature dependence in the fluorescence intensity ratio ($I_{monomer}/I_{excimer}$), especially in the high temperature range. Two separate films (thickness of (125 ± 2) nm) were prepared with significantly lowered BPP mass fractions of 0.001 and 0.01. The film with a BPP mass fraction of 0.001 did not yield measurable temperature dependence in the fluorescence intensity ratio above than the background noise. The film with a BPP mass fraction of 0.01 exhibited measurable temperature dependence in the fluorescence intensity ratio similar to those shown in *Fig. 5*. However, the signal level dropped to the background noise level after the first heating cycle. This limited success with 0.01 mass fraction of chromophore suggests, nonetheless, that the viscosity of the surrounding polystyrene chains, even in samples with a BPP mass ratio of up to 0.1, controls the dynamics of the BPP.

The thickness dependence of the operationally defined T_g is presented in *Fig. 6*. These data show no dependence on T_g for the range of thickness tested. This finding is consistent with the two previous studies using fluorescence probes (7, 8). It is also important to note that the present work was performed on a quartz substrate, while most previous work was conducted on silicon substrates. There may be subtle differences in the surface chemistry between the silicon substrate of previous studies and the quartz substrate of this study, and this may account for the discrepancy between our results and those observed by others (3–6). Experiments to determine the CTE of polystyrene supported on quartz substrates are currently under way and will be reported in the near future (27).

SUMMARY

The excimer fluorescence technique for measurement of T_g in of ultra-thin films has been demonstrated in this study. In this technique, the intensity of the excimer emission wavelength of the probe molecule is sensitive to the change in the polymer matrix viscosity. By measuring the ratio of the intensity of two wavelengths corresponding to different configurations of the probe molecule, an estimate of the relative local viscosity can be determined. The data exhibit two distinct regions of temperature behavior: a lower temperature, temperature-independent region and a higher temperature, temperature-dependent region. The transition between these two observed behaviors occurs at the macroscopically measured T_g for the polymer matrix. A linear extrapolation method from each of these two regions was employed to give an operational definition of the glass transition temperature.

This technique has been applied to five spun-cast polystyrene films supported on quartz with thicknesses ranging from 200 nm down to 25 nm. The thicknesses of the films were determined using by X-ray reflectivity. Multiple determinations of the T_g were performed with both heating and cooling temperature cycles. There was no observable shift in the T_g with replicate determinations.

The mean value of the T_g determined for each of the five polystyrene films was identical within the experimental uncertainty, and this value was also identical to that of the DSC measured T_g for the polymer matrix.

REFERENCES

1. Semetec, *National Semiconductor Roadmap* (1998).
2. R. Dias, D. Goyal, S. Tandon and G. Samelson. *Analytical Challenges in Next Generation Packaging/Assembly*, 1–591, AIP Press, Woodbury, New York (1998).
3. J. A. Forrest, K. Dalnoki-Veress and J. R. Dutcher, *Physical Review E*, **56**, 5705 (1997).
4. C. W. Frank, V. Rao, M. M. Despotopoulou, R. F. W. Pease, W. D. Hinsberg, R. D. Miller and J. F. Rabolt, *Science*, **273**, 912–15 (1996).
5. W. Wallace, J. H. vanZanten and W. L. Wu, *Phys. Rev. E.*, **52**, R3329 (1995).
6. J. H. vanZanten, W. Wallace and W. L. Wu, *Phys. Rev. E.*, **53**, R2053 (1996)
7. D. B. Hall, J. C. Hooker and J. M. Torkelson, *Macromolecules*, **30**, 667–69 (1997).
8. D. B. Hall, R. D. Miller and J. M. Torkelson, *J. Polymer Science B. Polymer Physics*, **35**, 2795–2802 (1997).
9. J. G. Victor and J. M. Torkelson, *Macromolecules*, **20**, 2241–50 (1987).
10. M. M. Despotopoulou, R. D. Miller, J. F. Rabolt and C. W. Frank, *J. Polymer Science B: Polymer Physics*, **34**, 2335–49 (1996).
11. C. S. P. Sung and N. H. Sung, *Materials Science and Engineering*, **A162**, 241–47 (1993).
12. K. E. Miller, R. H. Krueger and J. M. Torkelson, *J. Polymer Science Part B. Polymer Physics*, **33**, 2343–49 (1995).
13. K. A. Zachariasse, G. Duveneck and R. Busse, *J. Am. Chem. Soc.*, **106**, 1045 (1983).
14. K. A. Zachariasse, R. Busse, G. Duveneck and W. Kuhnle, *J. Photochem*, **28**, 237 (1985).
15. K. A. Zachariasse, W. Kuhnle, U. Leinhos and P. Reynders, *J. Phys. Chem.*, **95**, 5476 (1991).
16. A. J. Bur, F. W. Wang, C.L.Thomas and J. L. Rose, *Polymer Engineering and Science*, **34**, 671 (1994).
17. K. B. Migler and A. J. Bur, *Poly. Eng. and Sci.*, **38**, 213–21 (1998).
18. D. P. Jing, L. Bokobza, L. Monnerie, P. Collart and F. C. Deschryver, *Polymer*, **31**, 110–14 (1990).
19. D. P. Jing, L. Bokobza, P. Sergot, L. Monnerie, P. Collart and F. C. Deschryver, *Polymer*, **30**, 443–46 (1989).
20. L. Bokobza, C. Phamvancang, L. Monnerie, J. Vandendriessche and F. C. Deschryver, *Polymer*, **30**, 45–50 (1989).

21. Identification of a commercial product is made only to facilitate experimental reproducibility and to describe adequately experimental procedure. In no case does it imply endorsement by NIST or imply that it is necessarily the best product for the experiment.
22. W. M. Prest and D. J. Luca, *J. Applied Physics.*, **50**, 6067–71 (1979).
23. W. M. Prest and D. J. Luca, *J. Applied Physics.*, **51**, 5170 (1980).
24. J. D. Keddie, R. A. Jones and R. A. Cory, *Europhysics Letters*, **27**, 59–64 (1994).
25. L. Xie, G. B. Demaggio, W. E. Frieze, J. Devries, D. W. Gidley, H. A. Hristov and A. F. Yee, *Physical Review Letters*, **74**, 4947–50 (1995).
26. Y. Liu, T. P. Russel, M. G. Samat, J. Stohr, H. R. Brown, A. Cossy-Favre and J. Diaz, *Macromolecules*, **30**, 7768–71 (1997).
27. C. C. White and W.-L. Wu, submitted to *Polym. Eng. Sci.* (2001).